This is an Accepted Manuscript of a book chapter published by Routledge/CRC Press in **Trends in Maritime Technology and Engineering** on **June 7, 2022**, available online: https://www.routledge.com/Trends-in-Maritime-Technology-and-Engineering-Proceedings-of-the-6th-International/Soares-Santos/p/book/9781032335742

Postprint of: Wołoszyk K., Garbatov Y., Numerical modelling and analysis of steel specimens subjected to marine immersed corrosion and tensile load, Trends in Maritime Technology and Engineering, Vol. 1 (2022), pp.243-248, DOI: 10.1201/9781003320272-27

Numerical modelling and analysis of steel specimens subjected to marine immersed corrosion and tensile load

K. Woloszyk
Institute of Ocean Engineering and Ship Technology, Gdansk University of Technology, Narutowicza 11/12 st., 80-233, Gdansk, Poland

Y. Garbatov
Centre for Marine Technology and Ocean Engineering (CENTEC), Instituto Superior Técnico, University of Lisbon, Avenida Rovisco Pais, 1049-001 Lisboa, Portugal

ABSTRACT: The present study develops numerical models to analyse the behaviour of steel specimens subjected to marine immersed corrosion degradation and tensile load. The Finite Element Method with the use of the explicit dynamic solver LS-DYNA, satisfying the quasi-static conditions, is employed. Two numerical models are developed, where in the first one, the scans of surfaces gathered from corroded plate specimens are implemented directly to the finite element model. In the second one, the corroded surfaces are generated using random fields. Three different plate thicknesses are investigated. The mechanical properties, i.e., yield stress, Young's modulus, ultimate tensile stress, and total elongation, of specimens subjected to tensile loading for each numerical model are analysed. The results are validated against the experimental test, and failure modes are compared. It was found that both numerical models can estimate the mechanical properties of the corroded plate specimens and are very close to those of the experiment test. Thus, the random field modelling was very efficient in generating the real corroded plate surfaces of analysed specimens.

1 INTRODUCTION

Marine structures operating in a sea environment are subjected to corrosion degradation, which could significantly deteriorate the ultimate strength of structural elements (Garbatov, *et al.*, 2017; Woloszyk, *et al.*, 2018). Two and most important phenomena will govern the structural degradation. First, on a macro-scale, the thickness will be nonuniformly reduced, whereas the localised nonuniformities in corroded surfaces on a micro-scale will cause the reduction of mechanical properties (Garbatov, *et al.*, 2014).

The degradation problem of marine structures was investigated by various studies, accounting for different corrosive mediums. A Series of experiments in marine immersed corroded specimens, accelerated with the application of electric current were performed in (Garbatov, *et al.*, 2014, 2018), accounting also for different cleaning methods. The reduction of mechanical properties with corrosion degradation development was evident. However, after cleaning, the surface of specimens became smoother, and the reduction of properties was smaller. The tensile tests of naturally corroded specimens in atmospheric conditions were performed in (Qin, *et al.*, 2016; Wang, *et al.*, 2017; Nie, *et al.*, 2019; Xu, *et al.*, 2019), leading to similar conclusions. It needs to be noted that yield stress and ultimate tensile stress were reduced, but total elongation decreased even more significantly.

Apart from experiments, numerical simulations were performed too. Wang et al. (2017) measured the actual topography of corroded specimens and implemented it in the FE model, and the agreement with experiments was good. Recently, the random field approach was adopted to model the topography of corroded specimens (Woloszyk and Garbatov, 2020b, 2020a) and was found to be a very efficient tool compared to the one of performing real corrosion testing.

The present study compares different modelling techniques that could be adopted in corrosion degradation modelling of small-scale specimens subjected to tensile loading. Two different models are considered, i.e., corrosion fields are based on the scanning of corroded specimens and generated randomly. The results are compared with experimental tests described in (Woloszyk, *et al.*, 2021), where the analysed specimens were subjected to marine immersed corrosion degradation performed in an accelerated manner in the laboratory (Woloszyk, *et al.*, 2021). Compared to previous studies, the corrosion was accelerated by controlling only natural corrosion degradation factors.

2 EXPERIMENTS

The specimens were made of mild steel, and three different thicknesses were considered, namely 5 mm, 6 mm, and 8 mm.

The tensile tests were performed according to ISO norm (ISO, 2009). The standard coupon specimens were fabricated with the dimensions presented in Figure 1.

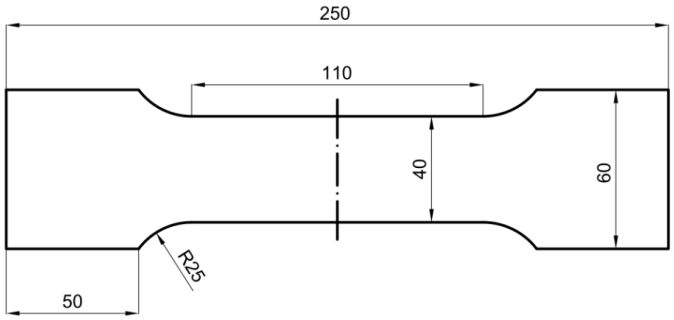

Figure 1. Steel specimen.

The initial mechanical properties (for non-corroded material) were determined for each plate thickness as presented in Table 1, where the mean values are obtained from testing six specimens for each thickness.

Table 1. Mechanical properties of non-corroded plates.

Thickness [mm]	Young modulus $E\ [Gpa]$	Yield stress $R_e\ [MPa]$	Ultimate tensile stress $R_u\ [MPa]$	Total elongation $\delta\ [-]$
5	197.4	272.3	389.2	0.266
6	196.4	284.4	410.3	0.260
8	199.1	360.6	465.2	0.219

Further, ten specimens of each thickness were subjected to marine immersed corrosion degradation. The corrosion testing set-up and results were described broadly in (Woloszyk, *et al.*, 2021). Nevertheless, the main features are also briefly introduced here.

The coupon specimens were corroded in approx. 900-litre tank fabricated from GRP laminate together with stiffened plates of a larger size. The corrosion rate was controlled by amplifying natural corrosion degradation factors only, without applying an electric current. Thus, the temperature was increased by the heating system, oxygen content by aeration and water velocity by circulation pumps. The achieved mean corrosion rates were 0.649 mm/year, 1.009 mm/year and 1.025 mm/year for 5 mm, 6 mm and 8 mm specimens, respectively (Woloszyk, *et al.*, 2021).

After corrosion degradation, the specimens were cleaned and scanned. The example of a specimen during scanning is presented in Figure 2.

Figure 2. Cleaned specimen (Woloszyk, *et al.*, 2021).

The results of scanning, including detailed statistics regarding the topography of corroded surfaces (mean value, standard deviation, etc.), are given in (Woloszyk, *et al.*, 2021). Due to their extensivity, they are not given here directly to keep the presented work's consistency. The obtained 3D surfaces were further applied in the FE model. Ten specimens were subjected to corrosion degradation for each thickness, leading to degradation levels as presented in Table 2.

Table 2. Degree of Degradation levels of corroded specimens.

Specimen number	Degree of Degradation level [%]		
	5 mm plates	6 mm plates	8 mm plates
No. 1	3.2	2.2	1.7
No. 2	5.9	6.3	4.0
No. 3	7.4	6.8	12.3
No. 4	8.0	9.6	13.8
No. 5	13.1	12.3	14.1
No. 6	15.4	14.1	14.8
No. 7	15.4	14.7	15.6
No. 8	15.5	16.6	16.9
No. 9	16.0	17.6	18.4
No. 10	24.3	21.3	28.4

The corroded specimens were also subjected to tensile testing, and mechanical properties were determined, as given in (Woloszyk, *et al.*, 2021). The results of experiments are used in current work to validate the numerical approaches.

3 FINITE ELEMENT MODELING

3.1 *Basic information*

The computations were carried out using Ansys LS-Dyna (ANSYS Inc., 2019) explicit dynamic solver with the satisfaction of quasi-static conditions. In comparison to an implicit solver, the explicit solver

doesn't face convergence problems. As for the finite elements, the SOLID164 elements were used.

In terms of constitutive law, the multilinear material model was adopted. Primarily, the engineering stress-strain response of the intact specimen needs to be similar in terms of both experiment and numerical simulations. To achieve that, the true stress-strain relationship needs to be incorporated in the FE code:

$$\varepsilon_{true} = \ln(1+\varepsilon) \quad (1)$$

$$\sigma_{true} = \sigma(1+\varepsilon) \quad (2)$$

where σ and ε are engineering stress and strain, respectively.

The above formulations are valid up to the ultimate tensile strength point. Then, where the necking phenomenon starts to occur, and the power-law based procedure is introduced (Nutor, 2017):

$$\sigma_{true} = K\varepsilon_{true}^{n} \quad (3)$$

where n and K are the strain hardening parameter and strength coefficient, respectively.

The comparison between the engineering stress-strain curve for both experiment and FE model for 5 mm plates is presented in Figure 3. It is noted that both curves match very well, i.e., the actual stress-strain behaviour in material level was properly captured.

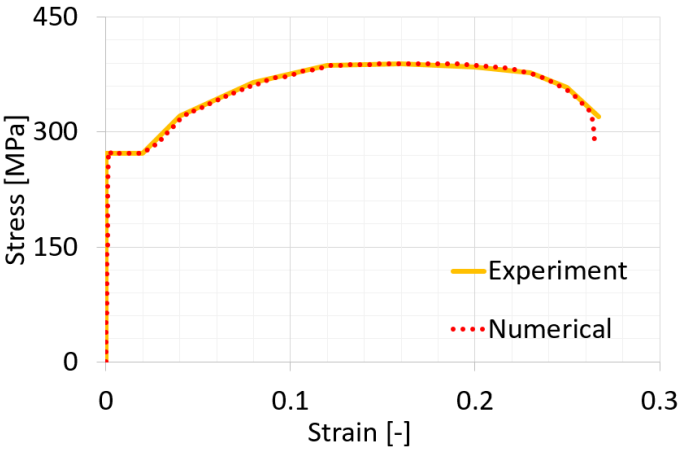

Figure 3. Engineering stress-strain curves of experimentally tested specimens and numerical simulations – 5 mm plates.

3.2 *Random field modelling*

Random field modelling as an approach to model the corrosion of small-scale specimens was proposed and discussed in (Woloszyk and Garbatov, 2020b, 2020a). The random field is the set of an infinite number of spatially correlated random variables. However, for engineering purposes, the discretised random fields are typically used specified by their mean value $\mu(\boldsymbol{x})$, variance $\sigma^2(\boldsymbol{x})$ and autocovariance function $C(\boldsymbol{x}, \boldsymbol{x}')$.

The autocovariance function governs the correlation level, and the most important parameter of it is the so-called correlation length. With the increase of correlation length, the correlation is extended, i.e., the field became smoother. Oppositely, the field is more irregular for lower correlation length.

In the current study, the Karhunen – Loeve expansion (Ghanem and Spanos, 1991) is used as the discretisation method. The MatLab software (MathWorks, 2019) was used to generate the random fields and specially developed code (Constantine, 2012), which allows generating a Gaussian random field for a specified mesh density and different correlation lengths. The calibration of the correlation length is based on the real corrosion degradation measurements. The example of an FE model with randomly generated surfaces of corrosion is presented in Figure 4.

Figure 4. FE model of the specimen with randomly generated random fields of corrosion.

4 RESULTS AND DISCUSSION

4.1 *Mechanical properties*

For each case presented in Table 2, the three runs of analysis with generated random fields are performed and mean values of mechanical properties are calculated. Compared to previous validation cases (Woloszyk and Garbatov, 2020b, 2020a), where atmosphericsally corroded specimens were analysed, the marine immersed corrosion brings strong correlated random fields. Thus, the correlation length of 10 mm was used in most cases, up to 17 mm for several ones. The maximum corrosion depth and mean corrosion depth were identical for each random field concerning the measured corrosion characteristics.

Figure 5 shows the obtained mechanical properties for various methods, considering 5 mm specimens. In general, the FE computations (both with exact and randomly generated corrosion fields) showed a higher decrease in mechanical properties. Since both FE models show very close results, the differences with the experiment are caused by the large scatter of mechanical properties in the non-corroded case. For example, the maximum observed yield stress was

higher by 30 MPa regarding the mean value (K Woloszyk, *et al.*, 2021). Thus, for several points, in an experimental domain, the observed mechanical properties in the corroded state were higher than the mean value in non-corroded specimens. A similar observation is captured in terms of ultimate tensile stress. There was no evident correlation between changes in Young's modulus and the degree of degradation.

Further, the experimentally obtained values were significantly higher concerning numerical ones. There are several possible reasons. Firstly, the extensometer could measure the strains inaccurately due to the un-uniformity of the corroded surfaces. Secondly, similarly to other mechanical properties, quite a high initial scatter was observed. Finally, the closest results between the exact FE model and experiment were obtained for total elongation, and in this case, the initial scatter of this property was not that high. However, the model with randomly generated corrosion fields showed an even higher decrease of that parameter.

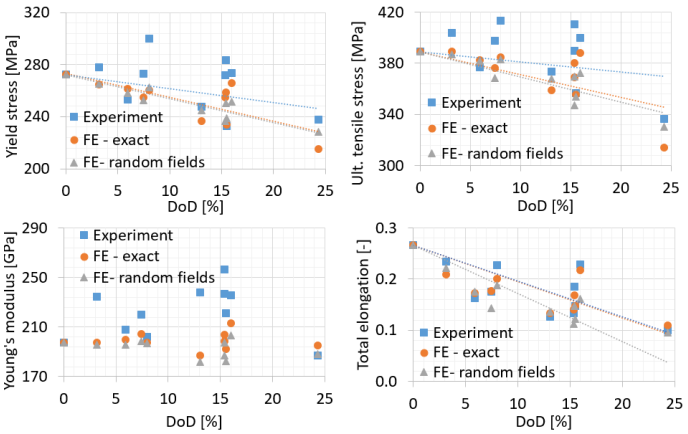

Figure 5. Mechanical properties for 5 mm specimens.

The changes in mechanical properties considering various models and 6 mm specimens are presented in Figure 6. From the beginning, it is noted that an excellent convergence has been obtained between numerical models. Thus, random fields accurately simulated the actual corrosion fields. Although a similar scatter of mechanical properties coming from tests has been visible as in the case of 5 mm specimens, the regressions were much closer between an experimental curve and FE computations, even though quite significant differences were visible for some points. However, in this case, the scatter was compensated. Thus, for some points, the observed experimental values were lower than numerical ones, and for some points, it was oppositely. In ultimate tensile stress and total elongation, the regressions were almost identical. Only in yield stress, a slightly higher decrease of this parameter with corrosion development was obtained via FE computations. Similarly, to 5 mm specimens, the unrealistic values of Young's modulus were obtained for several points in an experiment.

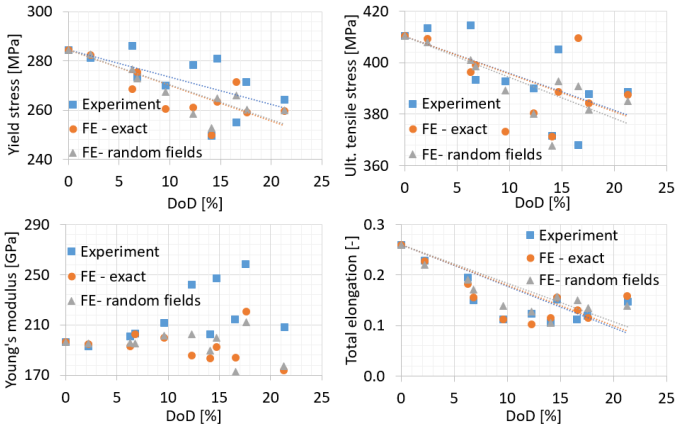

Figure 6. Mechanical properties for 6 mm specimens.

Figure 7 presents the results of mechanical properties changes for 8 mm specimens. It is noted that very close results in terms of particular points and regressions were observed for experiment and numerical models with exact fields of corrosion. In 8 mm specimens, the observed initial scatter of mechanical properties was the lowest within thicknesses. However, a lower decrease of mechanical properties was observed for the numerical model with randomly generated random fields of corrosion. This indicates that for some specimens, the actual corrosion characteristics were not modelled accurately. The observed values of Young's modulus between numerical models were rather similar. However, experimental results were significantly higher.

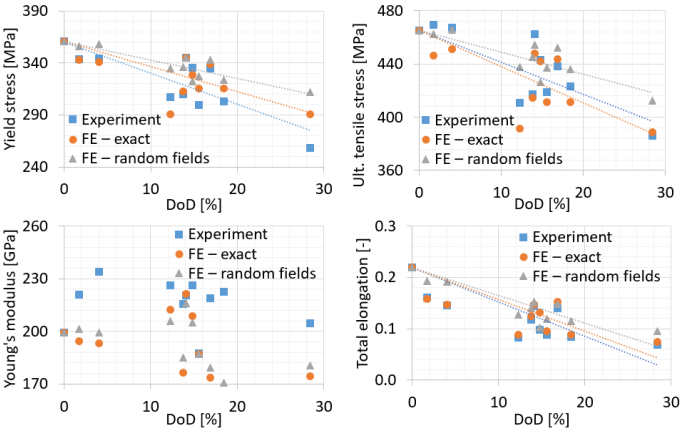

Figure 7. Mechanical properties for 8 mm specimens.

It was also observed that the scatter of mechanical properties was not significantly smaller in comparison to experimental results. This indicates that not only initial uncertainty of mechanical properties, but corrosion too, brings variability in the obtained results.

4.2 *Failure modes*

The comparison between failure modes of tested specimens and FE computations with measured corrosion fields for two selected specimens is presented in Figures 8 and 9.

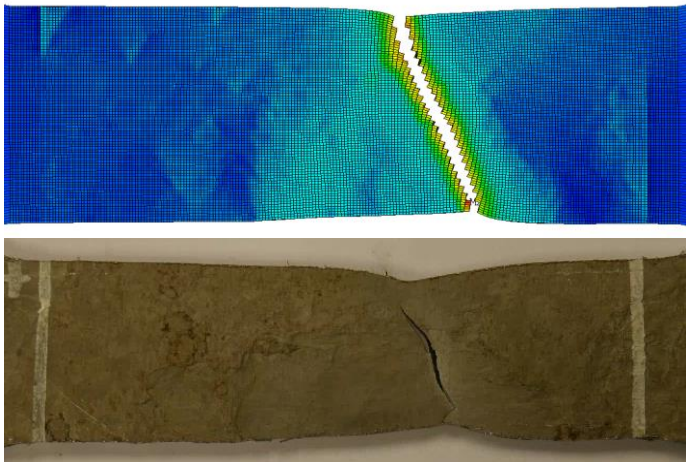

Figure 8. Comparison between failure modes in FE model and experiment for selected 6 mm specimen.

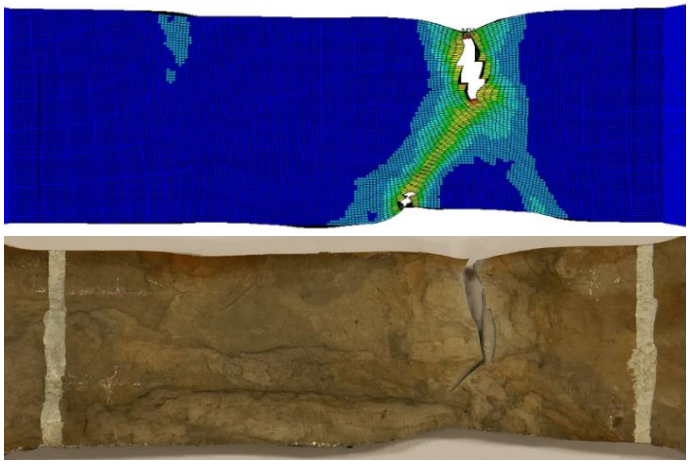

Figure 9. Comparison between failure modes in FE model and experiment for selected 8 mm specimen.

It is noted that in both cases (Figures 8 and 9), the failure positions have been identical. Further, the exact failure behaviour has been captured as well. In the case of a 6 mm specimen (Figure 8), the breaking line was inclined concerning the longitudinal direction of the specimen. In the case of an 8 mm specimen, the breaking initiated from the upper edge of the specimen almost perpendicularly to the longitudinal direction. Further, the breaking line was inclined. This indicates that the FE model could accurately predict corroded specimens' structural behaviour in marine immersed corrosion.

5 CONCLUSIONS

Based on the presented results, it could be concluded that the FE modelling is very efficient to predict the decrease of mechanical properties with corrosion degradation development. Major differences when comparing to experimental results are due to the significant scatter of mechanical properties of intact specimens as well as uncertainties due to surface characteristics of corroded specimens.

The random fields are very efficient in simulating the real corrosion characteristics, although, for 8 mm specimens, the lower decrease of mechanical properties has been observed compared to the FE model with exact corrosion fields adopted.

Random field modelling has another advantage. Using random field techniques, one can generate many samples, which is challenging in other cases due to the long duration of the corrosion degradation process and a very functional analysis of the corrosion morphology, and in this way, it is economically justified. Nevertheless, more experimental work should be done to validate the proposed methodology. The changes in the mechanical properties may vary depending on the corrosion type and other factors (marine, atmospheric, etc.).

6 ACKNOWLEDGEMENTS

This work has been supported by the National Science Centre, Poland (grant No. 2018/31/N/ST8/02380). Calculations were carried out at the Academic Computer Centre in Gdańsk.

7 REFERENCES

ANSYS Inc. (2019) 'ANSYS LS-DYNA User's Guide'.

Constantine, P. (2012) *Random Field Simulation*.

Garbatov, Y., Guedes Soares, C., Parunov, J. and Kodvanj, J. (2014) 'Tensile strength assessment of corroded small-scale specimens', *Corrosion Science*, 85, pp. 296–303.

Garbatov, Y., Saad-Eldeen, S., Guedes Soares, C., Parunov, J. and Kodvanj, J. (2018) 'Tensile test analysis of corroded cleaned aged steel specimens', *Corrosion Engineering, Science and Technology*. Taylor & Francis, pp. 1–9.

Garbatov, Y., Tekgoz, M. and Guedes Soares, C. (2017) 'Experimental and numerical strength assessment of stiffened plates subjected to severe non-uniform corrosion degradation and compressive load', *Ships and Offshore Structures*, 12(4), pp. 461–473.

Ghanem, R. G. and Spanos, P. D. (1991) *Stochastic Finite Elements: A Spectral Approach*, *Stochastic Finite Elements: A Spectral Approach*. New York, NY: Springer New York.

ISO (2009) 'Metallic materials - Tensile testing - Part 1: Method of test at room temperature.', *International Standard ISO 6892-1*.

Kwesi Nutor, R. (2017) 'Using the Hollomon Model to Predict Strain-Hardening in Metals', *American Journal of Materials Synthesis and Processing*, 2(1), pp. 1–4.

MathWorks (2019) 'MATLAB R2019b'.

Nie, B., Xu, S., Yu, J. and Zhang, H. (2019) 'Experimental

investigation of mechanical properties of corroded cold-formed steels', *Journal of Constructional Steel Research*. Elsevier, 162, p. 105706.

Qin, G., Xu, S., Yao, D. and Zhang, Z. (2016) 'Study on the degradation of mechanical properties of corroded steel plates based on surface topography', *Journal of Constructional Steel Research*, 125, pp. 205–217.

Wang, Y., Xu, S., Wang, H. and Li, A. (2017) 'Predicting the residual strength and deformability of corroded steel plate based on the corrosion morphology', *Construction and Building Materials*, 152, pp. 777–793.

Woloszyk, K. and Garbatov, Y. (2020a) 'An enhanced method in predicting tensile behaviour of corroded thick steel plate specimens by using random field approach', *Ocean Engineering*, 213, p. 107803.

Woloszyk, K. and Garbatov, Y. (2020b) 'Random field modelling of mechanical behaviour of corroded thin steel plate specimens', *Engineering Structures*, 212, p. 110544.

Woloszyk, K, Garbatov, Y. and Klosowski, P. (2021) 'Stress-strain model of lower corroded steel plates for fitness-for-purpose analyses', *Construction and Building Materials*, Submitted.

Woloszyk, Krzysztof, Garbatov, Y. and Kowalski, J. (2021) 'Indoor accelerated controlled corrosion degradation test of small- and large-scale specimens', *Ocean Engineering*, 241, p. 110039.

Woloszyk, K., Kahsin, M. and Garbatov, Y. (2018) 'Numerical assessment of ultimate strength of severe corroded stiffened plates', *Engineering Structures*, 168, pp. 346–354.

Xu, S., Zhang, H. and Wang, Y. (2019) 'Estimation of the properties of corroded steel plates exposed to salt-spray atmosphere', *Corrosion Engineering, Science and Technology*, 54(5), pp. 431–443.